Sensor and Simulation Notes

Note 121

November 1970

Electromagnetic Interaction Between a Cylindrical Post and a Two-Parallel-Plate Simulator, II (a Circular Hole in the Top Plate)

by

K. S. H. Lee

Northrop Corporate Laboratories
Pasadena, California

Abstract

The time history is obtained of the total current induced on a cylindrical post between a two-parallel-plate waveguide by a step-function plane wave traveling between the plates with a circular hole in the top plate coaxial with the post. By making such a hole it is possible to inhibit an intense electric field induced at the post's end.

The effect of the hole is also obtained on the lowest resonant frequency of the post and its associated peak current amplitude, the decay time constant and the peak current for a step-function incident wave.

Acknowledgment

Thanks are due to Mr. R. W. Sassman for his indispensable assistance in numerical computation, to Captain C. E. Baum for his many helpful suggestions, and to Mrs. G. Peralta for her help in typing the manuscript and preparing the figures.

I. Introduction

In a previous study of the electromagnetic interaction of a two-parallel-plate simulator and a post inside it, we have calculated the response of the post to a step-function incident plane wave traveling between the two plates.[1] Particular attention has been given to the effect of the plate spacing, for a given post length, on (a) the resonant frequencies and their associated peak current amplitudes of the post and (b) the decay time constant, the peak current, and the maximum electric field strength at the post's end for a step-function incident wave. We have found that this maximum electric field is, as expected, more enhanced the closer the post's end is to the top plate. To inhibit an intense field one may think of making a hole in the top plate coaxial with the post. Such an idea will obviously work, but it is not clear to what extent the other aforementioned quantities will be affected by such a hole. In this note, we will provide quantitiative information on these quantities, in addition to the maximum electric field at the post's end.

In section II, we derive all the necessary mathematical formulas for numerical calculations, which are carried out in section III. Most numerical results obtained in section III are graphed and some are tabulated. In section IV, the results of this note and two previous ones (Refs. 1 and 2) are summarized in tabular form for easy comparison.

II. Coupled Integral Equations

In this section we will derive all the necessary mathematical formulas that will be used in subsequent numerical computation.

Figure 1 is divided into two spatial regions: region (1) is defined by $z > s$, $\rho \geq 0$; region (2) is defined by $s > z > 0$ and outside the post. Since we are concerned with the total axial current on the post, we may restrict our consideration to the axisymmetric mode of the TM mode, i.e., the mode with nonvanishing components E_z, E_ρ and H_ϕ that are independent of ϕ. In region (1) we will express $H_\phi^{(1)}$ in terms of E_ρ in the circular hole with an appropriate Green's function. In region (2) we will write, with another appropriate Green's function, $H_\phi^{(2)}$ in terms of the incident field H_ϕ^{inc}, E_ρ in the hole, and $H_\phi^{(2)}$ on the post's surface. By letting the observation point lie on the post's surface we will obtain the first of the coupled integral equations for the unknowns E_ρ in the hole and $H_\phi^{(2)}$ on the post's surface. The other equation is gotten by equating $H_\phi^{(1)}$ to $H_\phi^{(2)}$ in the hole.

We now proceed to write down various mathematical expressions mentioned above with the aid of equation (A.7) in Reference 1, taking the post and the plates to be perfectly conducting. In region (1)

$$H_\phi^{(1)}(\rho,z) = -\,i\omega\varepsilon \int_0^b E_\rho(\rho',s)G_1(\rho,z;\rho',s)\rho' d\rho' \tag{1}$$

where G_1 satisfies the equation

$$\left[\frac{\partial^2}{\partial\rho^2} + \frac{1}{\rho}\frac{\partial}{\partial\rho} - \frac{1}{\rho^2} + \frac{\partial^2}{\partial z^2} + k^2\right]G_1 = -\,\delta(z - z')\,\frac{\delta(\rho-\rho')}{\rho'} \tag{2}$$

together with the radiation condition at infinity and the boundary condition $(\partial/\partial z)G_1 = 0$ for $z = s$. In region (2) we have

$$H_\phi^{(2)}(\rho,z) = H_\phi^{inc}(\rho) + \int_0^h \left[H_\phi^{(2)} \frac{\partial}{\partial\rho'}(\rho' G_2)\right]_{\rho'=a} dz'$$

$$+ \int_0^a d\rho'\rho' \left[H_\phi^{(2)} \frac{\partial G_2}{\partial z'}\right]_{z'=h} + i\omega\varepsilon \int_0^b d\rho'\rho' E_\rho(\rho',s)G_2(\rho,z;\rho',s) \tag{3}$$

provided that G_2 satisfies the same equation as G_1 with boundary conditions $(\partial/\partial z)G_2 = 0$ for $z = s$ and $z = 0$. Letting the observation point lie on the post's surface in (3), noting that $H_\phi^{inc}(\rho) = -iH_o J_1(k\rho)$, and defining $I(z) = 2\pi a H_\phi^{(2)}(a,z)$, $I_e(\rho) = 2\pi\rho H_\phi^{(2)}(\rho,h)$ we get

$$\frac{1}{2} I(z) + \int_o^h K(a,z;a,z')I(z')dz' - a \int_o^a I_e(\rho')\left[\frac{\partial G_2}{\partial z'}\right]_{z'=h} d\rho'$$

$$- 2\pi i\omega\varepsilon a \int_o^b d\rho'\rho' E_\rho G_2(a,z;\rho',s) = - 2\pi i a H_o J_1(ka) \quad ,$$

$$h \geq z \geq 0 \qquad (4)$$

Equating (1) to (3) in the hole ($z = s$, $b > \rho > 0$) we obtain

$$\int_o^h K(\rho,s;a,z')I(z')dz' - a \int_o^a d\rho' I_e(\rho')\left[\frac{\partial G_2}{\partial z'}\right]_{z'=h,z=s}$$

$$- 2\pi i\omega\varepsilon a \int_o^b d\rho'\rho' E_\rho(\rho')\left[G_1(\rho,s;\rho',s) + G_2(\rho,s;\rho',s)\right] = - 2\pi i a H_o J_1(k\rho) \quad ,$$

$$b \geq \rho \geq 0 \quad . \qquad (5)$$

Equations (4) and (5) are the coupled integral equations for $I(z)$ on the post and $E_\rho(\rho)$ in the circular hole. The quantities I_e, G_1, G_2 and K can be found in Reference 2 and are given below for easy reference:

$$I_e(\rho) = I(h)[1 - (1 - \rho^2/a^2)^{2/3}]$$

$$G_1(\rho,z;\rho',z') = \int_o^{2\pi} d\phi \cos\phi \left[\frac{e^{ikR_{-1}^{(+)}}}{4\pi R_{-1}^{(+)}} + \frac{e^{ikR_o^{(-)}}}{4\pi R_o^{(-)}}\right]$$

$$G_2(\rho,z;\rho',z') = \int_o^{2\pi} d\phi \cos\phi \sum_{m=-\infty}^{\infty}\left[\frac{e^{ikR_m^{(+)}}}{4\pi R_m^{(+)}} + \frac{e^{ikR_m^{(-)}}}{4\pi R_m^{(-)}}\right]$$

$$K(\rho,z;a,z') = -\left[\frac{\partial}{\partial\rho'}(\rho' G_2)\right]_{\rho'=a}$$

$$R_m^{(+)} = [(2ms + z + z')^2 + \rho^2 + \rho'^2 - 2\rho\rho' \cos\phi]^{\frac{1}{2}}$$

$$R_m^{(-)} = [(2ms - z + z')^2 + \rho^2 + \rho'^2 - 2\rho\rho' \cos\phi]^{\frac{1}{2}}$$

III. Numerical Results

As stated in the Introduction, the objective of studying this problem is to investigate what effect a circular hole in the top plate may have on the following quantities of importance: (i) the first resonant frequency and the associated peak current amplitude, (ii) the decay time constant and the peak current for a step-function incident wave, and (iii) the maximum electric field strength at the post's end for a step-function incident wave. For this purpose, the following values of parameters were chosen for study:

$a/h = .1, .01$

$h/s = .8;\ b/h = 0, 1/4, 1/2, 3/4, 1$
$h/s = .6;\ b/h = 0, 1/3, 2/3, 1$
$h/s = .4;\ b/h = 0, 1/2, 1$
$h/s = 0$ (free space)

(See Fig. 1 for the meaning of these parameters.)

Our point of departure is equations (4) and (5). They were solved on an electronic computer for the above values of parameters. For a step-function incident wave whose magnetic field vector is

$$\underset{\sim}{H}^{inc}(x,t) = -\underset{\sim}{e}_y H_o U(t - x/c) \quad ,$$

transient solutions were obtained by numerically performing Fourier inversion on the harmonic solutions of equations (4) and (5). From a study of the numerical results it was found that in the cases where $h/s = .6$ and $.4$, a hole as large as $b/h = 1$ in the top plate would not have appreciable effect on the important quantities mentioned above; that is to say, these quantities do not appreciably differ from the values corresponding to the case without any hole in the top plate. This is the reason why we give, in the following, curves almost exclusively for the case $h/s = .8$ with the hole radius as a parameter.

Figures 2 and 3 give the frequency variations of the post current at $z = 0$, showing that neither the first resonant frequency nor the peak current amplitude is affected appreciably by making a hole as large as $b/h = 1$ in the top plate.

In Figs. 4 and 5 are given the variations of the currents along the post around the first resonant frequency. The peak current is tabulated in Table I for various hole radii.

Table I. Current amplitude (at $z = 0$) at $k_o h = 1.3$ for $a/h = .1$ and at $k_o h = 1.5$ for $a/h = .01$ ($h/s = .8$).

	$a/h = .1$	$a/h = .01$
b/h	$\|I(0)\|/(hH_o)$	$\|I(0)\|/(hH_o)$
0	5.336	4.808
.25	5.305	4.867
.50	5.524	5.072
.75	5.759	5.300
1.00	5.954	5.444
Free Space	8.217	6.708

Note that the first free-space resonant frequency is given by $k_o h = 1.23$ for $a/h = .1$ and by $k_o h = 1.45$ for $a/h = .01$.

In Fig. 6a through Fig. 9b we plot the time histories of the induced current at $z = 0$ for a step-function incident wave. It can be seen that by making a larger hole in the top plate we can decrease the peak current, as expected. From these time-history curves we obtain the decay time constant τ_b, which is tabulated in Table II. Here, τ_b is measured in units of h/c and appears in the function e^{-t/τ_b}.

Table II. Decay time constant τ_b($h/s = .8$)

	$a/h = .1$	$a/h = .01$
b/h	τ_b/τ_o	τ_b/τ_o
0	.650	.611
.25	.617	.640
.50	.679	.705
.75	.622	.802
1.00	.764	.867

$$\tau_o = \text{decay time constant in free space} = \begin{cases} 4.732\ h/c \text{ for } a/h = .1 \\ 7.325\ h/c \text{ for } a/h = .01 \end{cases}$$

The approximate charge density on the post's end can be calculated from a knowledge of the current at the post's end, as has been shown in Ref. 2. Figures 10 and 11 give the frequency variations of C_k/C_o, where C_k and C_o are defined as follows:

$$\frac{|\sigma_o|}{\varepsilon_o E_o} = C_k(1 - \rho^2/a^2)^{-1/3}$$

$$C_s = \operatorname*{Limit}_{kh \to 0} C_k$$

$$C_o = \text{value of } C_s \text{ in free space} = \begin{cases} 9.72 \text{ for } a/h = .1 \\ 67.27 \text{ for } a/h = .01 \end{cases}$$

σ_o being the axisymmetric mode of the induced surface charge density on the post's end, E_o the electric field of the incident wave. When the incident wave is a step function, the time variation of $\sigma_o(\rho,t)$ is given in Figs. 12 and 13, where C_t is defined through the equation

$$\frac{\sigma_o(\rho,t)}{\varepsilon_o E_o} = C_t(1 - \rho^2/a^2)^{-1/3}$$

In Table III, we tabulate C_m/C_o (where C_m is the maximum value of C_t) together with C_s/C_o.

Table III. Surface charge density on the post's end (h/s = .8)

	a/h = .1		a/h = .01	
b/h	C_s/C_o	C_m/C_o	C_s/C_o	C_m/C_o
0	1.22	1.80	1.06	1.72
.25	1.12	1.61	1.02	1.67
.50	.97	1.41	.95	1.56
.75	.86	1.27	.87	1.43
1.00	.78	1.14	.80	1.32
Free Space	1.00	1.53	1.00	1.65

In the following concluding section we will summarize the results of this study and Refs. 1 and 2.

IV. Summary

We will summarize below, in Table IV, the findings of this and two previous studies on the following important quantities:

f_1 = lowest resonant frequency of the post current

I_1 = current amplitude at f_1 estimated at the post's base

τ_1 = decay time constant of the mode having resonant frequency f_1

i_m = peak current induced by a step-function incident wave at the post's base

σ_m = peak surface charge density on the post's end induced by a step-function incident wave

In Table IV, these quantities are normalized with respect to the corresponding quantities in free space, which are denoted by the subscript o.

Table IV. Summary of results

	PARALLEL PLATES WITH PROTRUDING POST (Ref. 1).	POST BETWEEN PARALLEL PLATES (Ref. 2).	POST BETWEEN PARALLEL PLATES WITH HOLE IN TOP PLATE (this note).
$\frac{f_1}{f_o}$	Increases toward unity with increasing hole size for fixed plate spacing	Insensitive to plate spacing.	Insensitive to the hole size for hole's radius as large as the post's length.
$\frac{I_1}{I_o}$	Decreases from unity with increasing hole size.	Increases with increasing plate spacing, reaches unity when s/h=2 for a/h=.1 and when s/h=1.6 for a/h=.01, and varies about unity for larger plate spacing with diminishing variations.	Same as f_1/f_o.
$\frac{\tau_1}{\tau_o}$	Increases toward unity with increasing hole size for fixed plate spacing. Decreases with increasing plate spacing for fixed hole size.	Increases with increasing plate spacing, reaches unity when s/h=2.1 for a/h=.1 and when s/h=1.7 for a/h=.01, and varies about unity for larger plate spacing with diminishing variations.	Increases with increasing hole size.
$\frac{i_m}{i_o}$	Decreases with increasing hole size for fixed plate spacing. Increases with increasing plate spacing for fixed hole size.	Independent of plate spacing.	Decreases with increasing hole size.
$\frac{\sigma_m}{\sigma_o}$	No information.	Decreases to unity with increasing plate spacing.	Same as i_m/i_o.

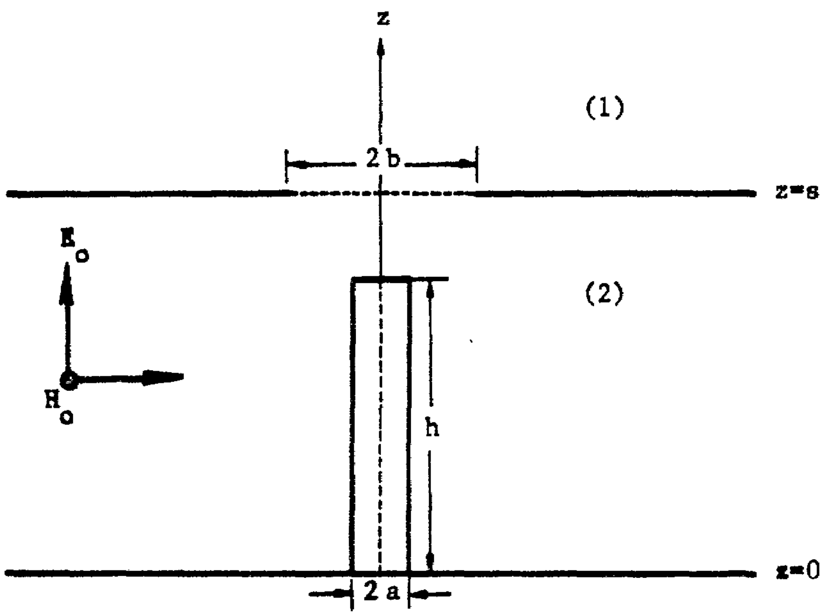

Figure 1. Side view of a cylindrical post within two parallel plates with circular hole in the top plate.

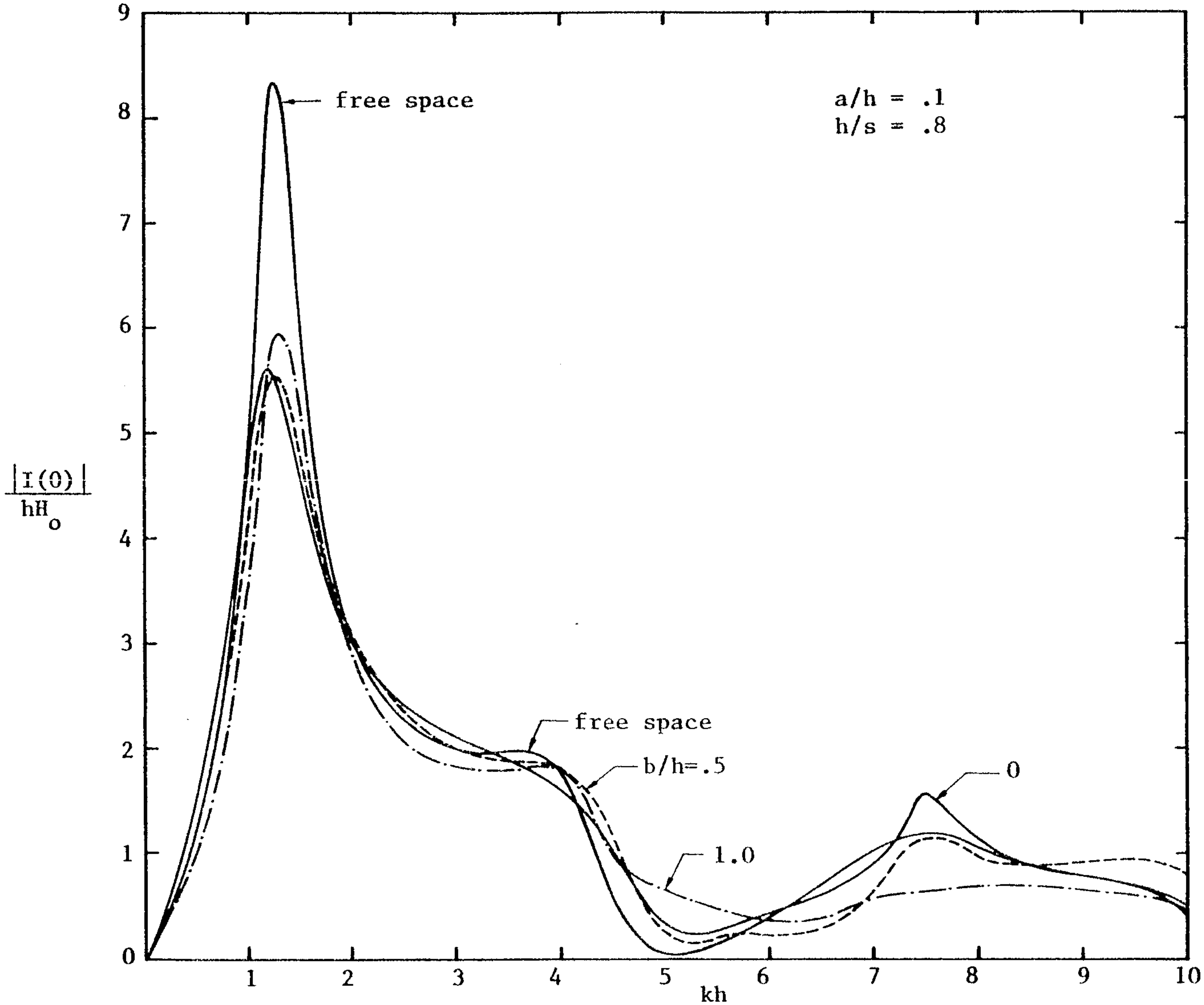

Figure 2. Frequency variation of post current at z=0 with hole radius as parameter.

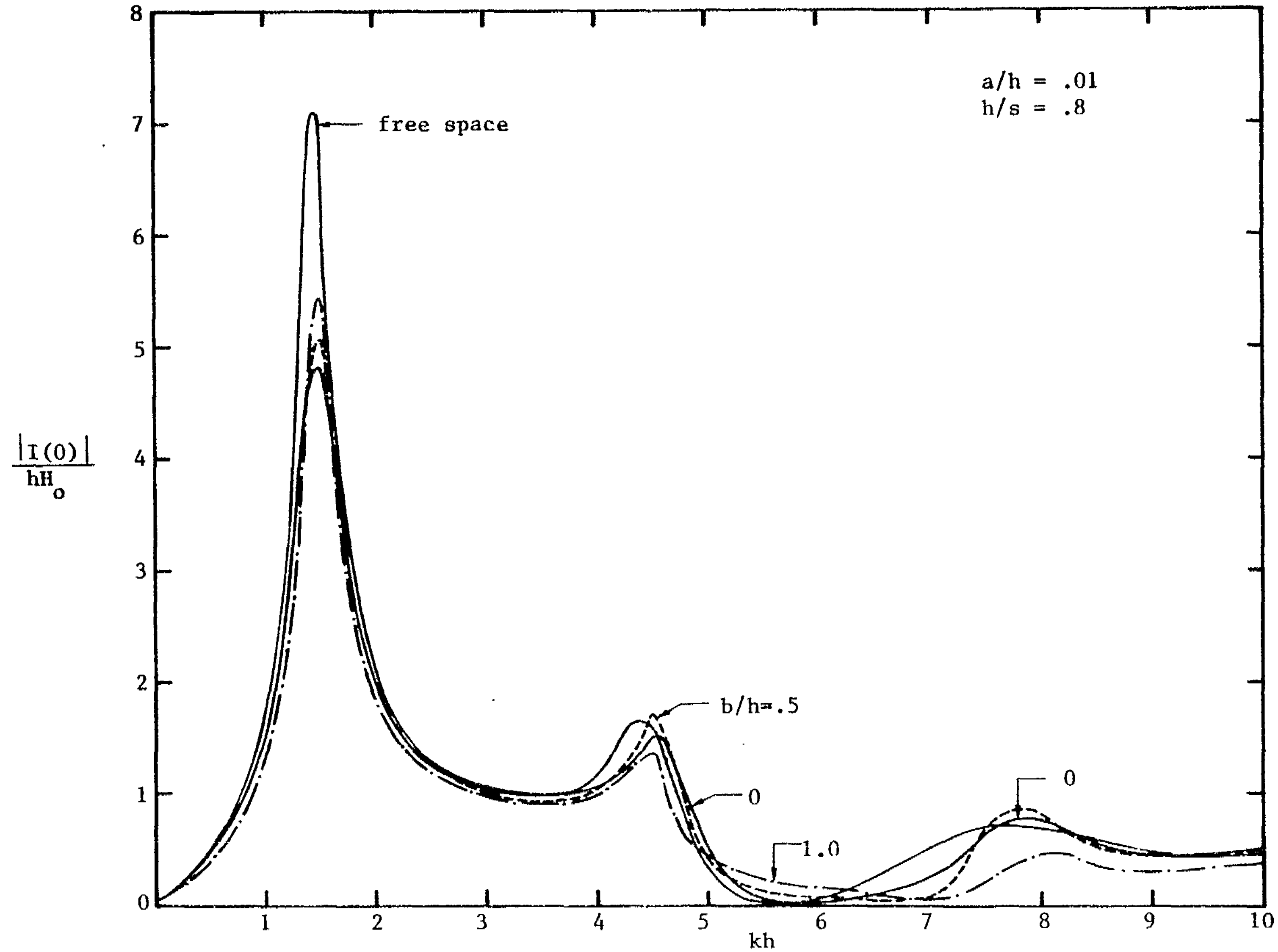

Figure 3. Frequency variation of post current at z=0 with hole radius as parameter.

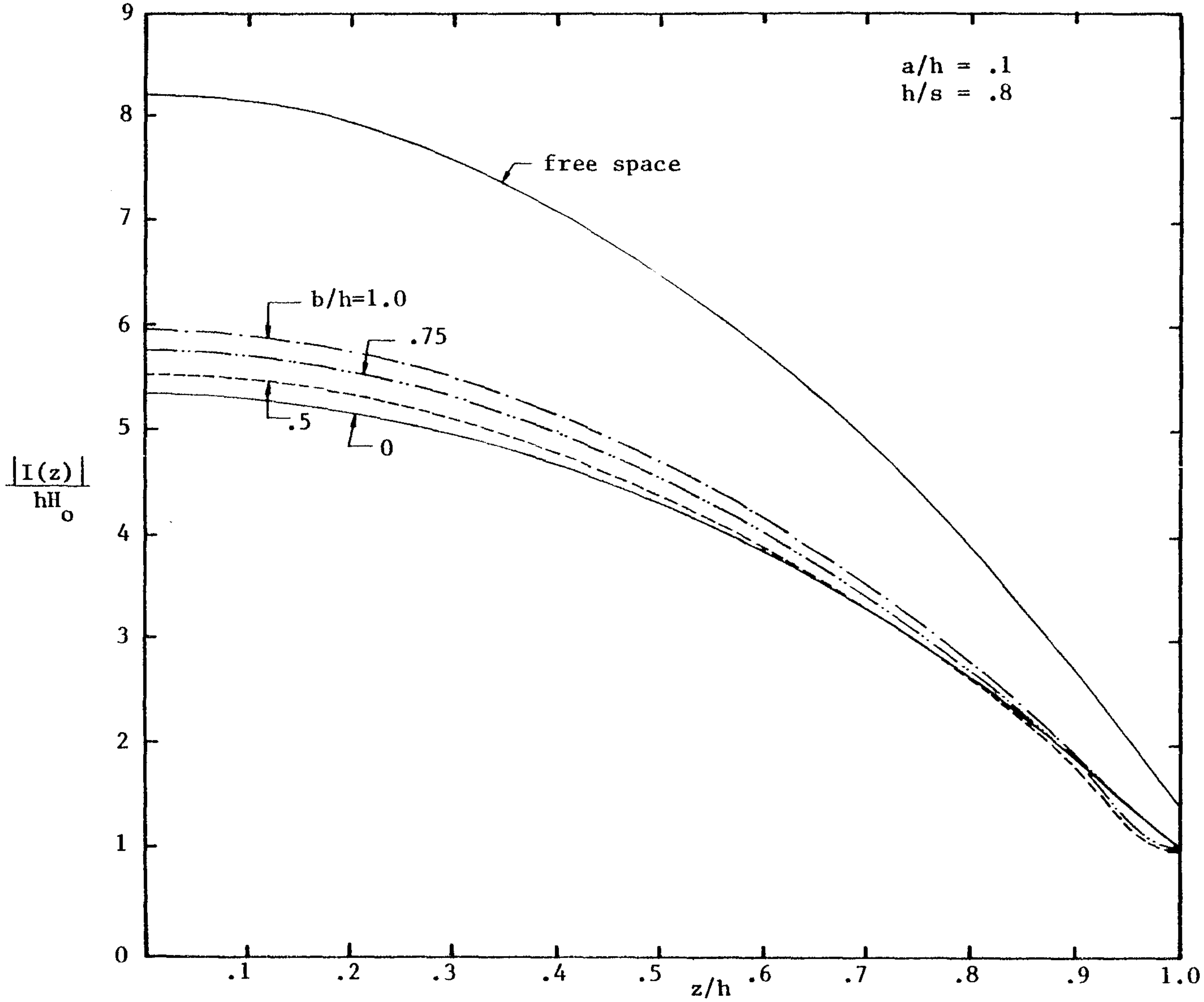

Figure 4. Current versus position at kh=1.3.
(Free-space first resonant frequency: $k_o h=1.23$)

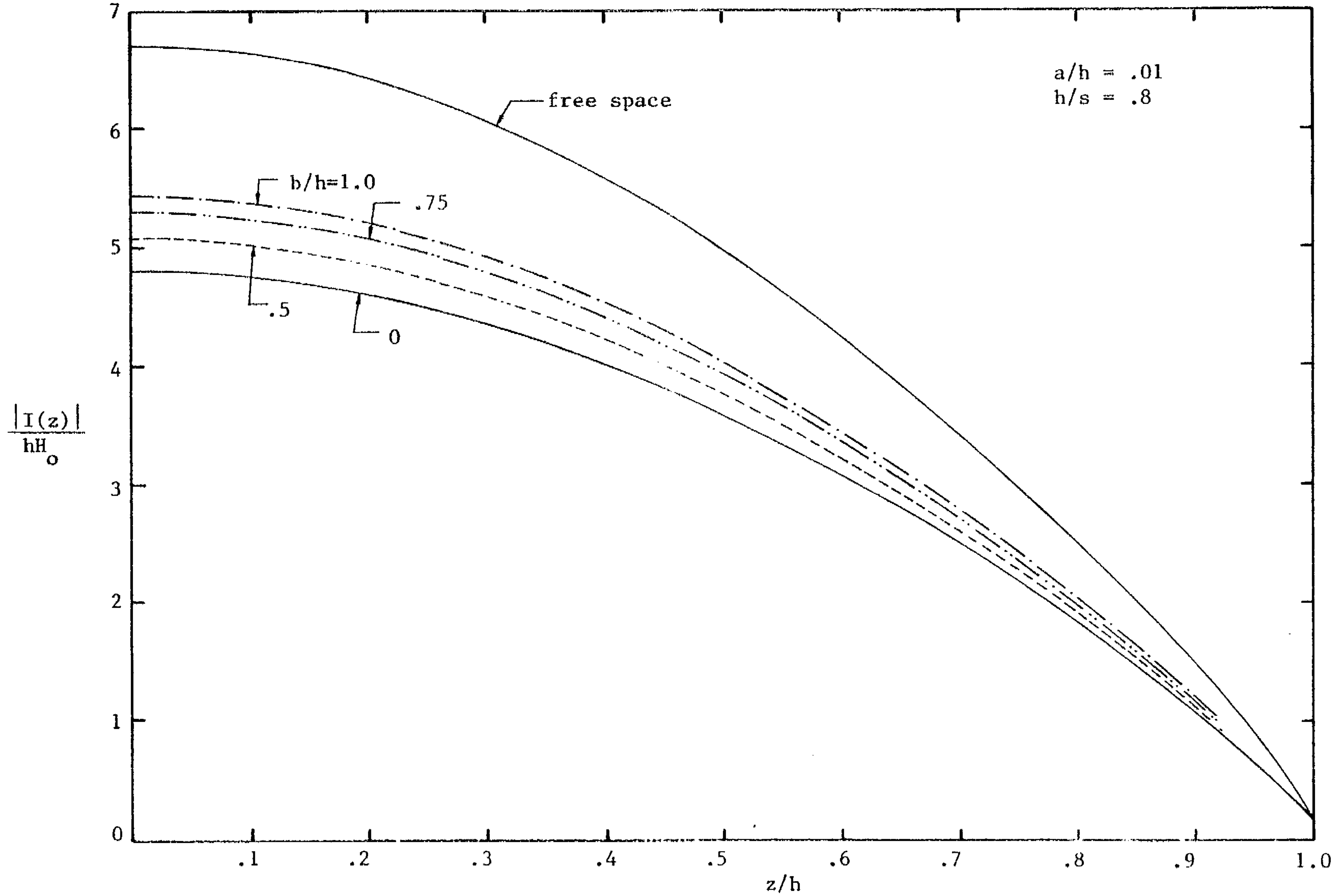

Figure 5. Current versus position at kh=1.5.(Free-space first resonant frequency: $k_o h=1.45$)

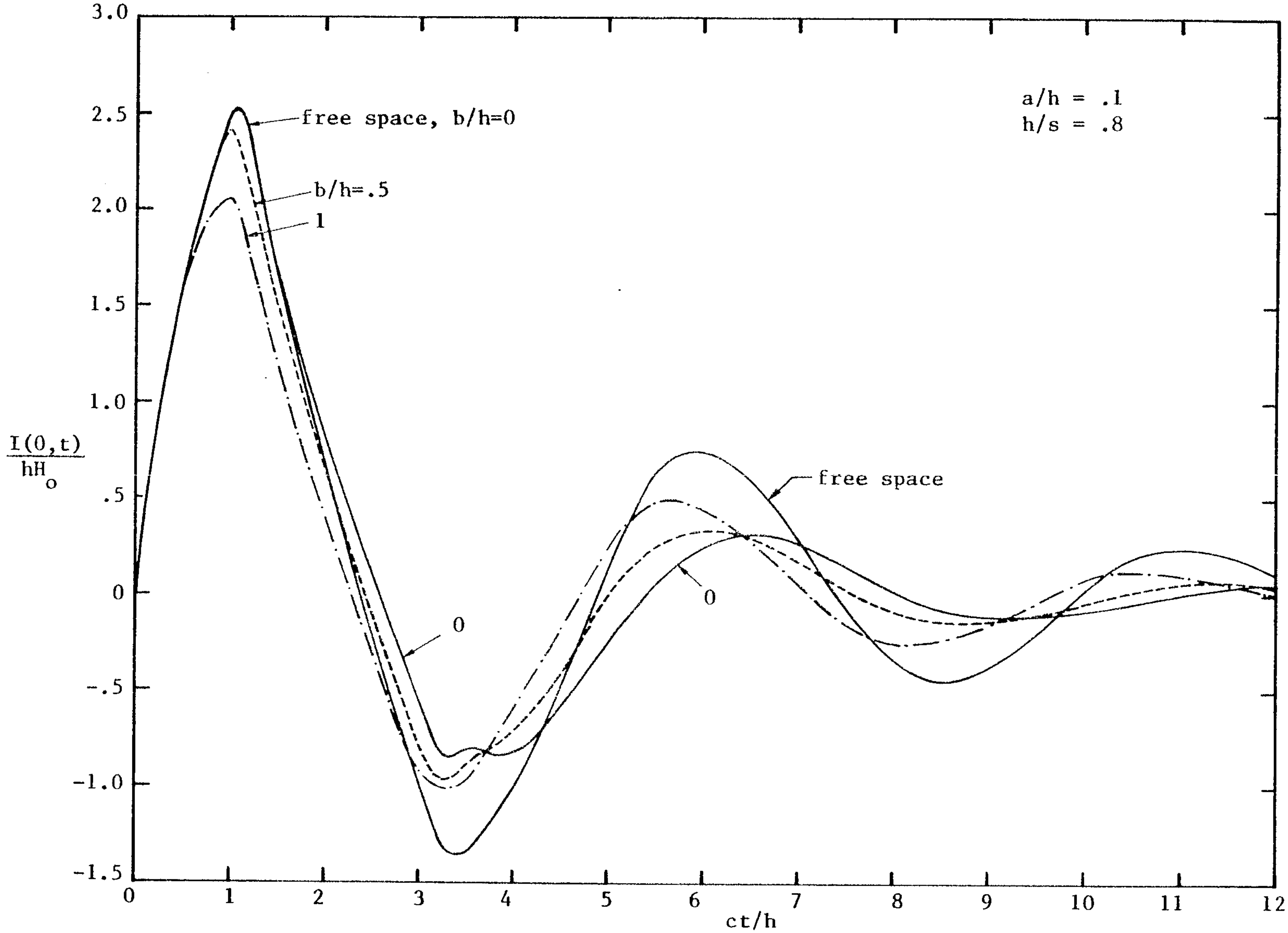

Figure 6a. Time history of post current at z=0 with hole radius as parameter.

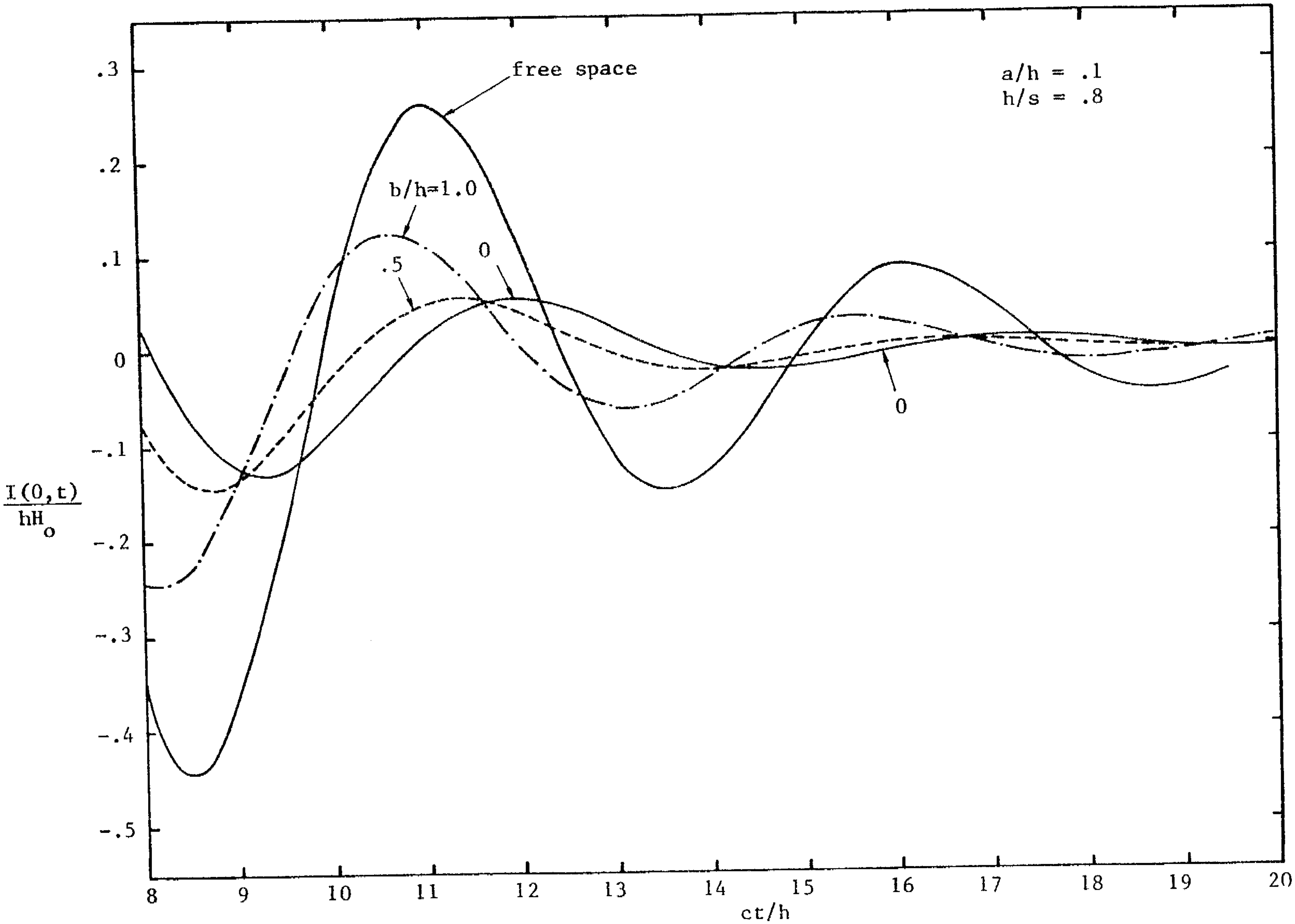

Figure 6b. Time history of post current at z=0 with hole radius as parameter.

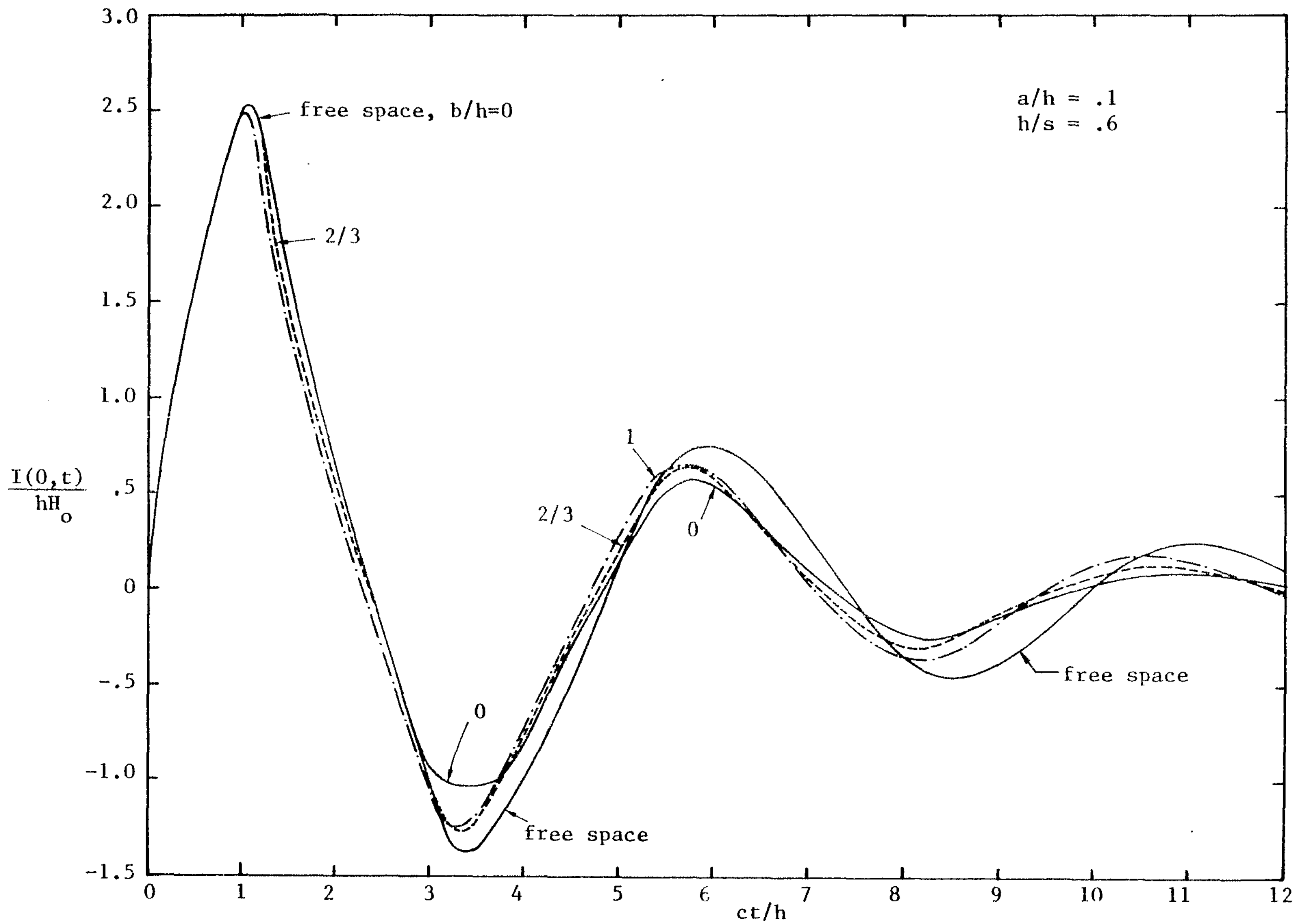

Figure 7a. Time history of post current at z=0 with hole radius as parameter.

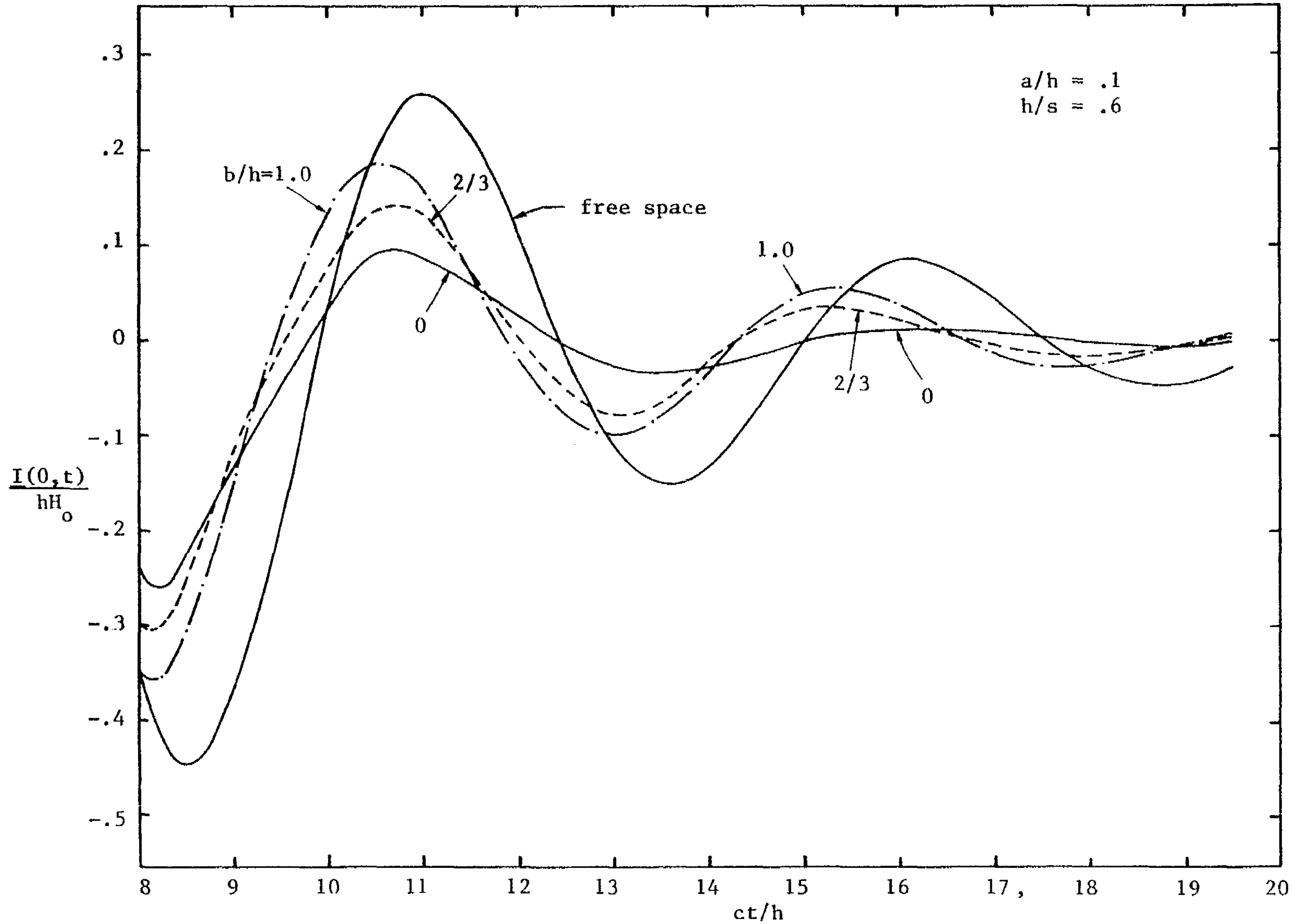

Figure 7b. Time history of post current at z=0 with hole radius as parameter.

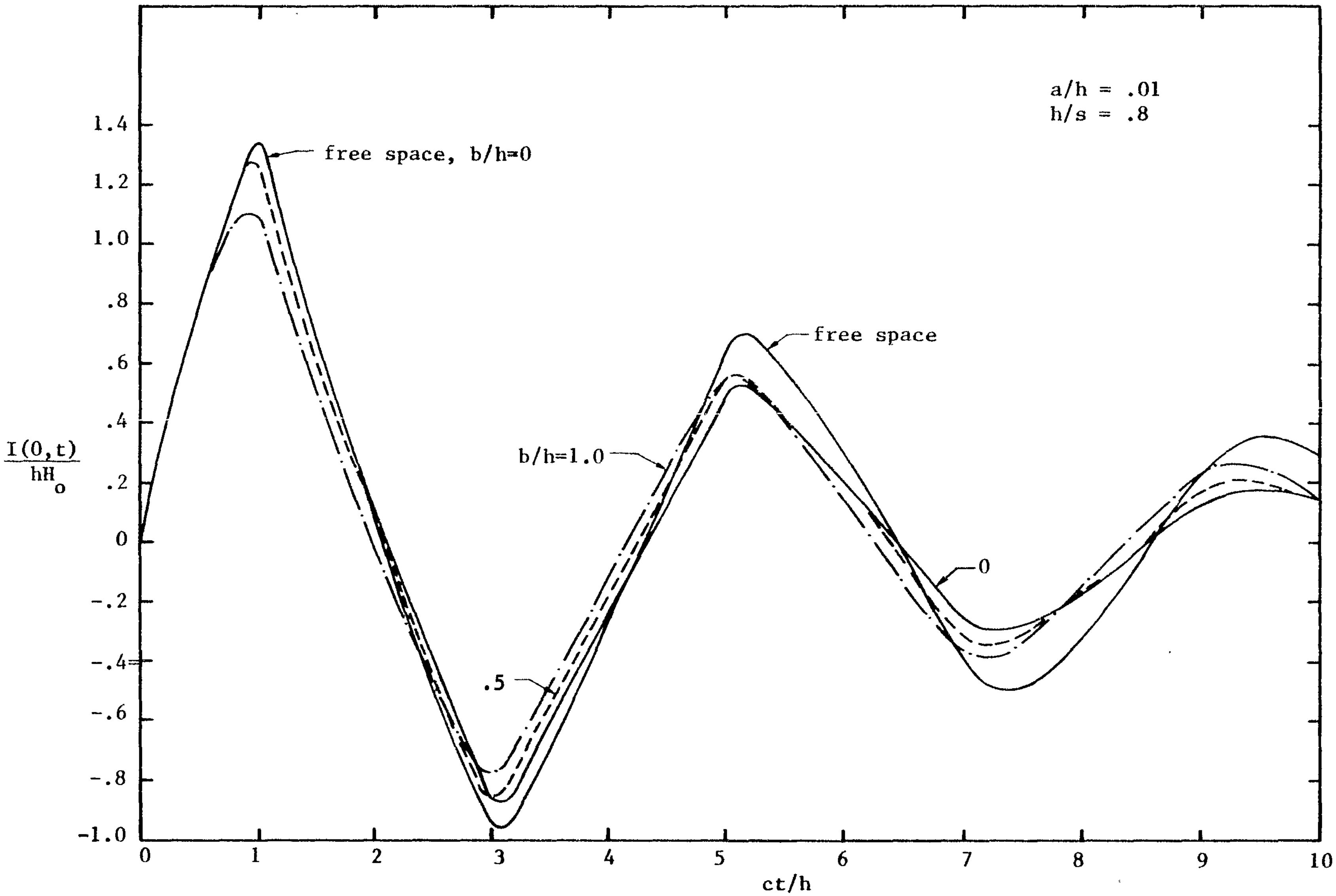

Figure 8a. Time history of post current at z=0 with hole radius as parameter.

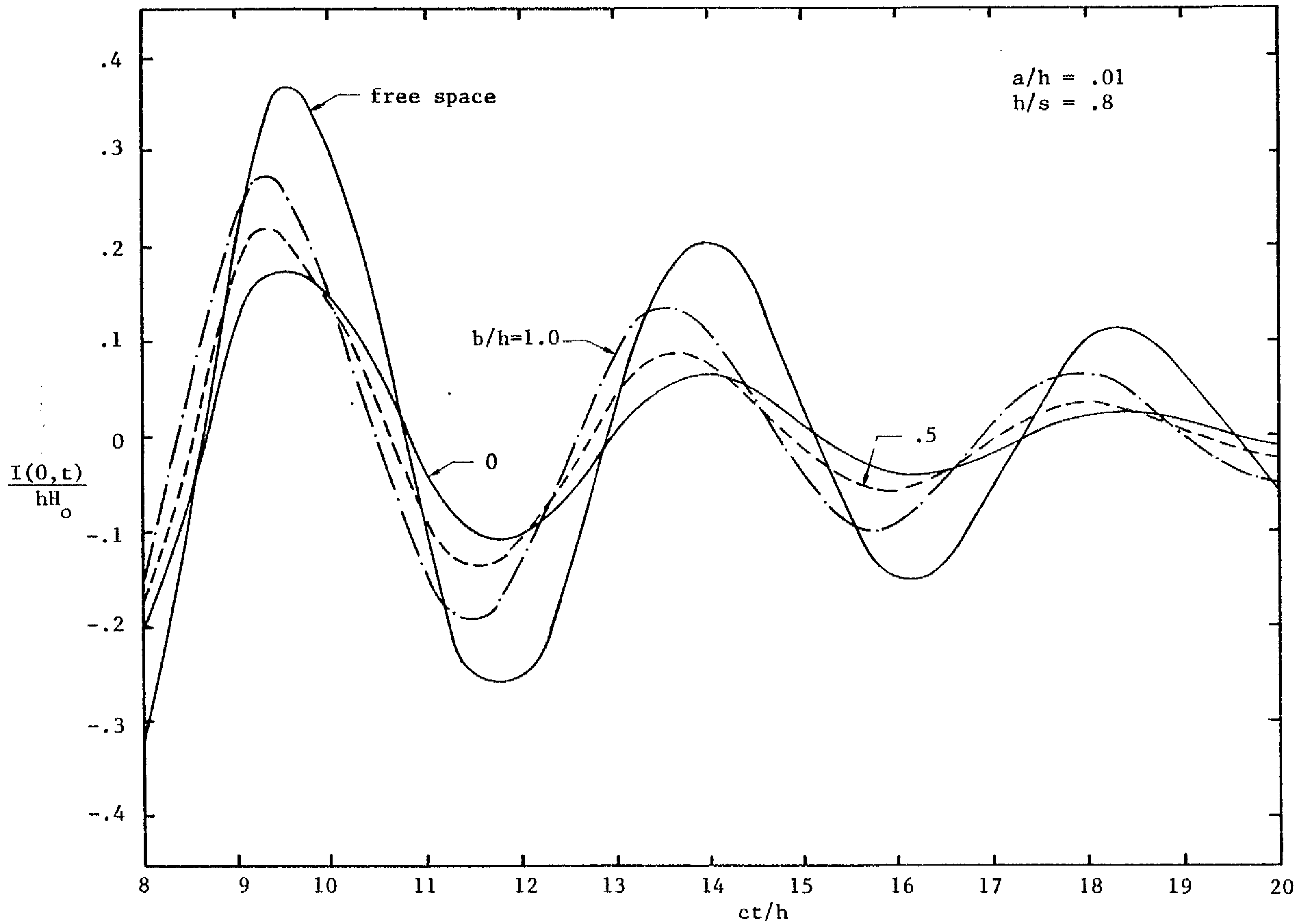

Figure 8b. Time history of post current at z=0 with hole radius as parameter.

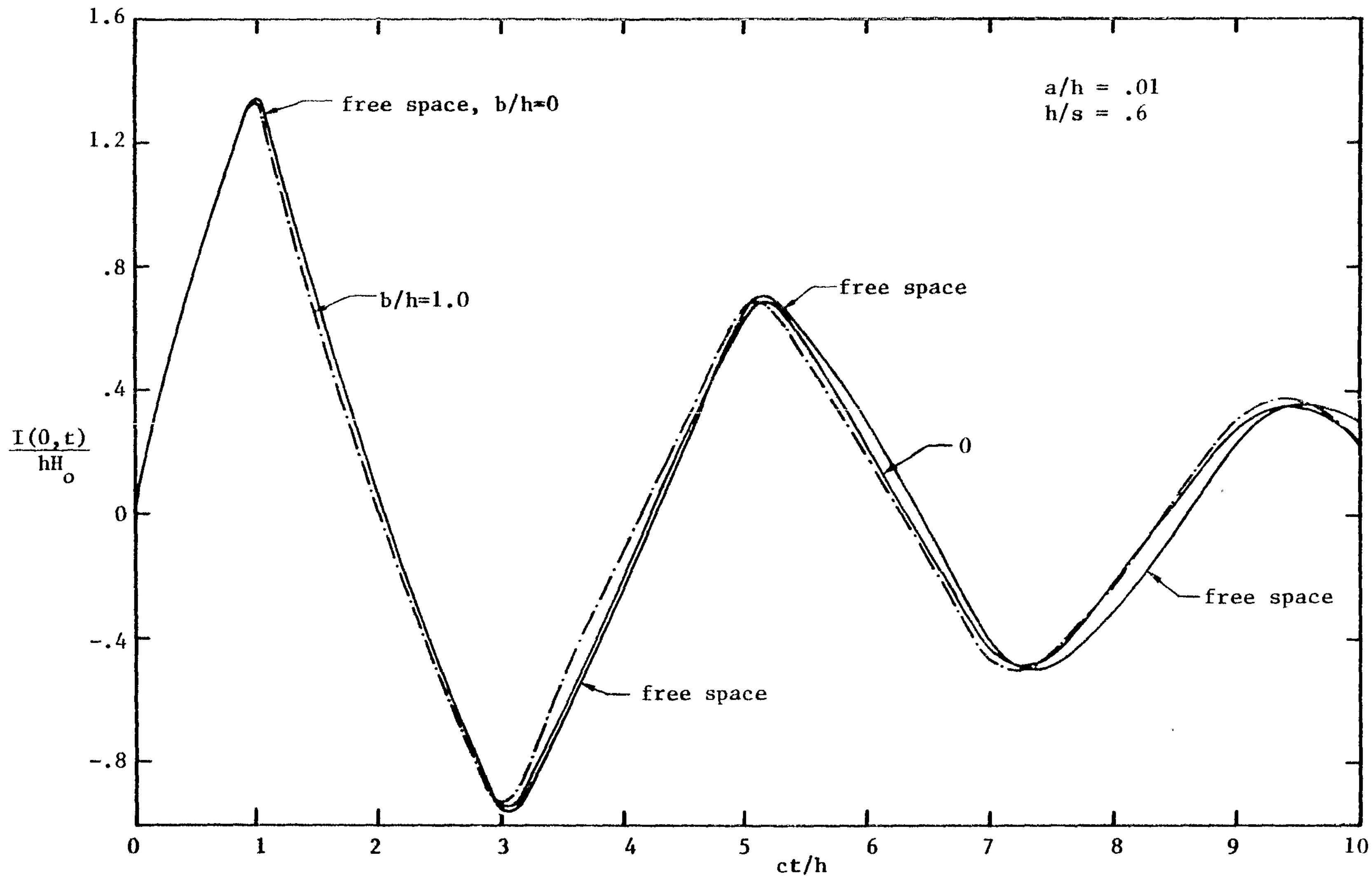

Figure 9a. Time history of post current at z=0 with hole radius as parameter.

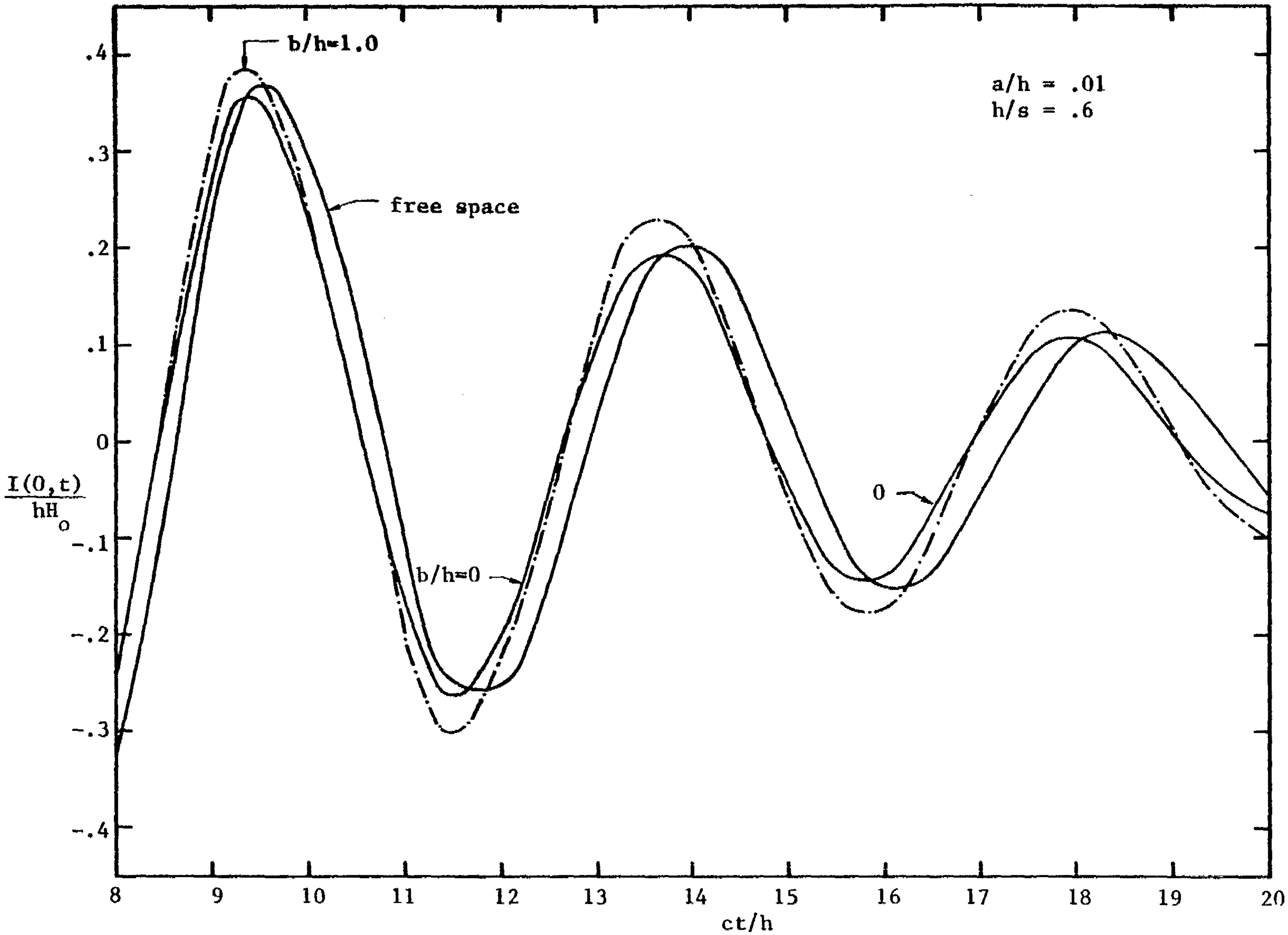

Figure 9b. Time history of post current at z=0 with hole radius as parameter.

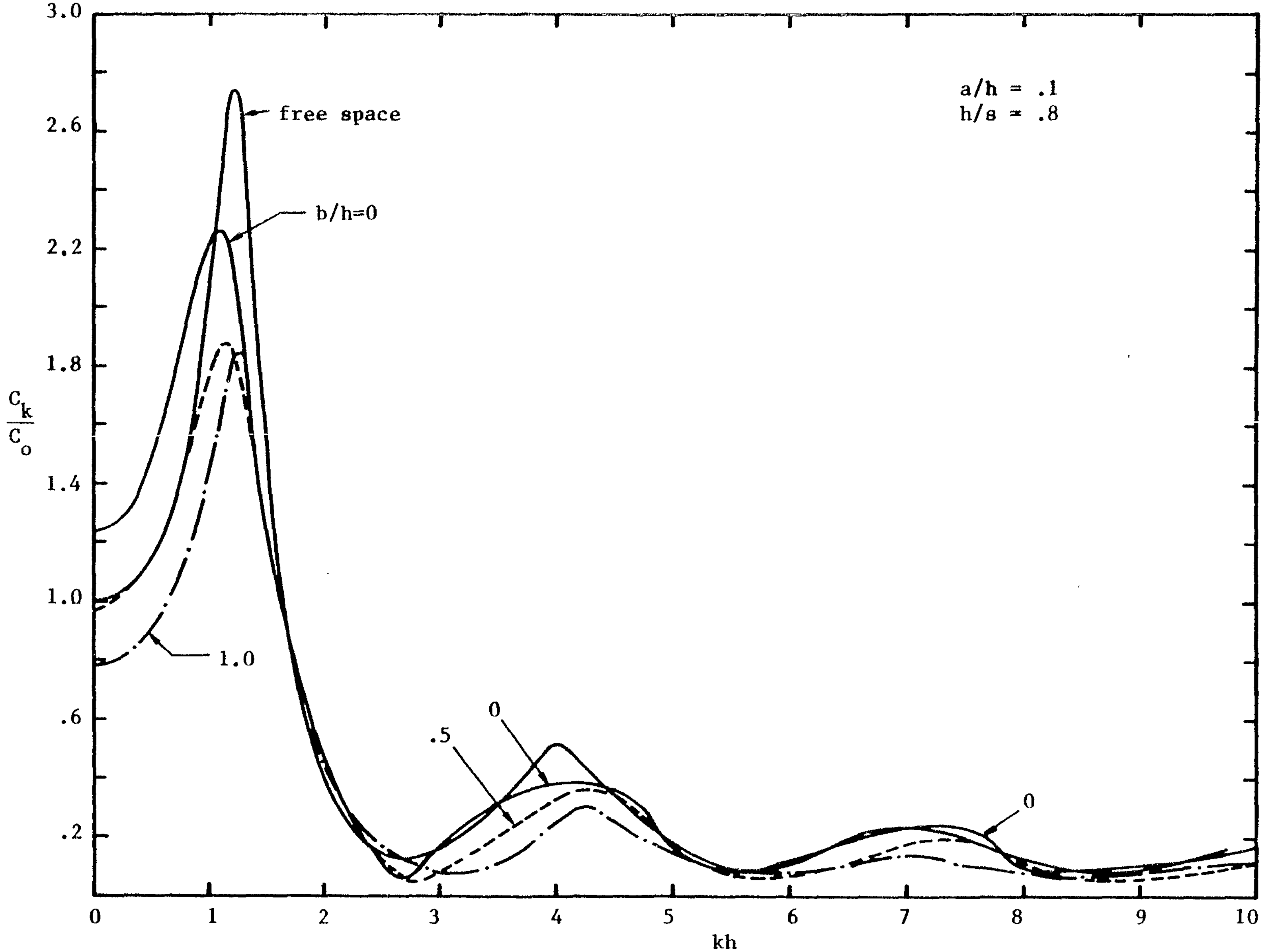

Figure 10. Frequency variation of surface charge density at the post's end with hole radius as parameter.

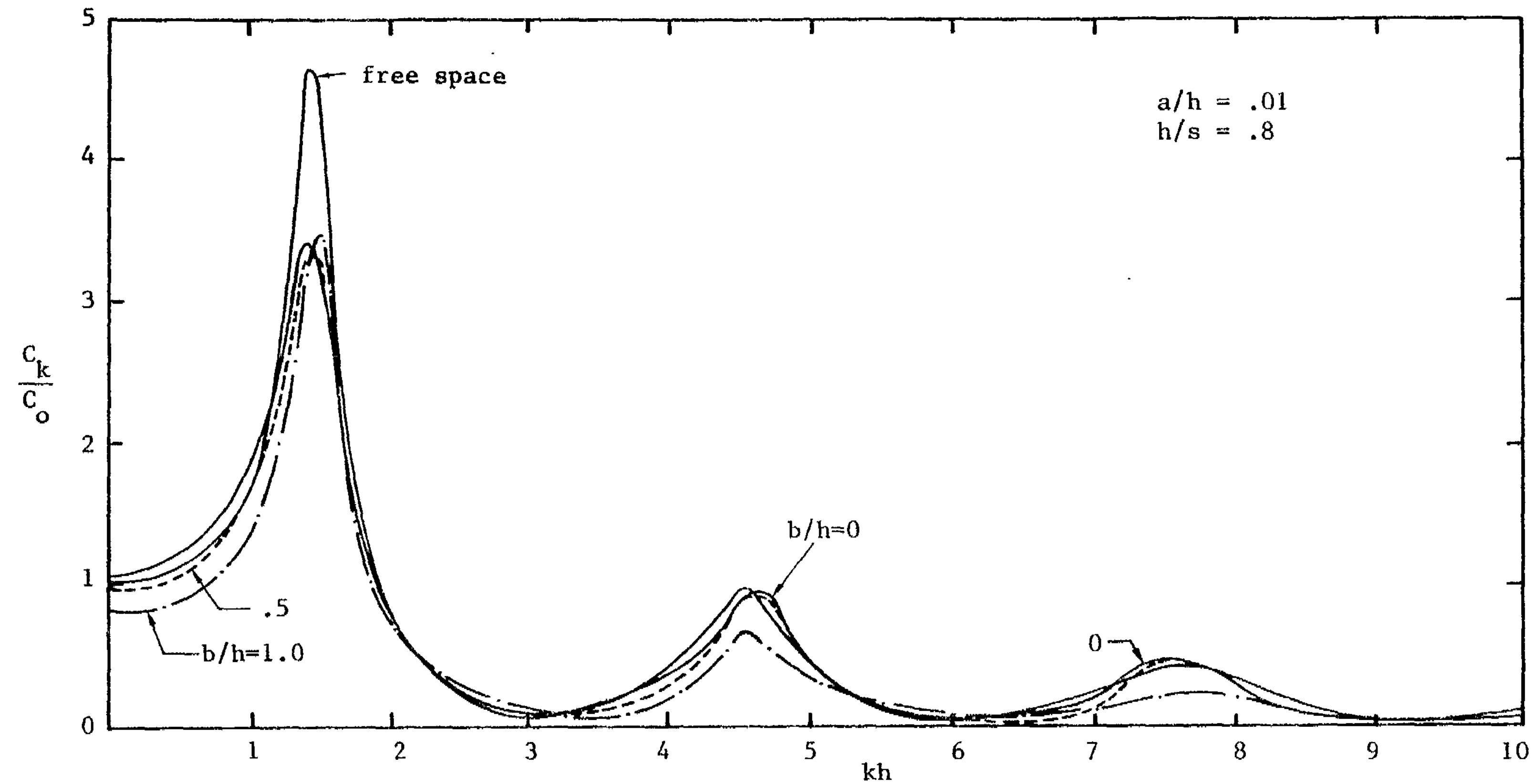

Figure 11. Frequency variation of surface charge density at the post's end with hole radius as parameter.

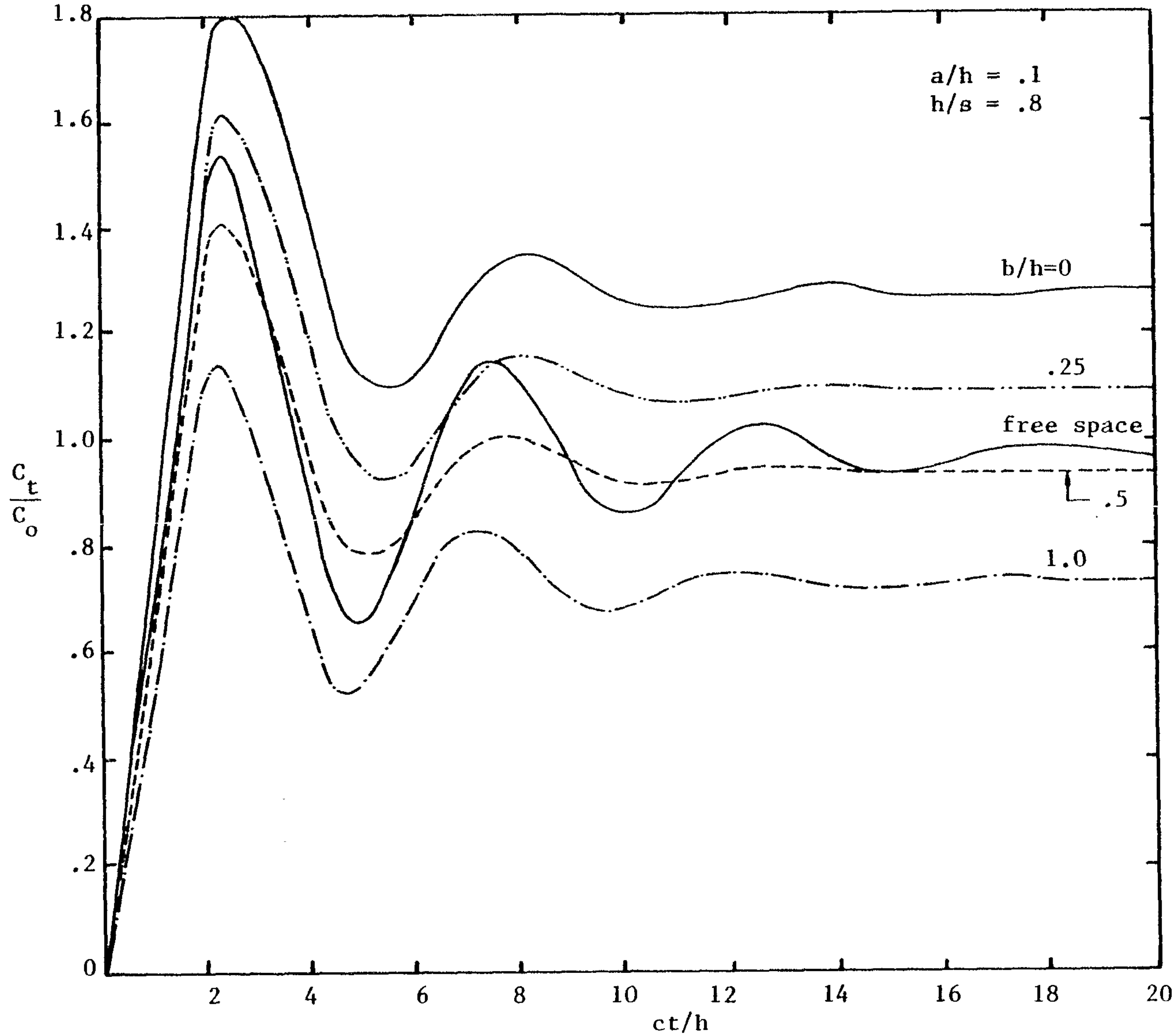

Figure 12. Time history of surface charge density at the post's end with hole radius as parameter.

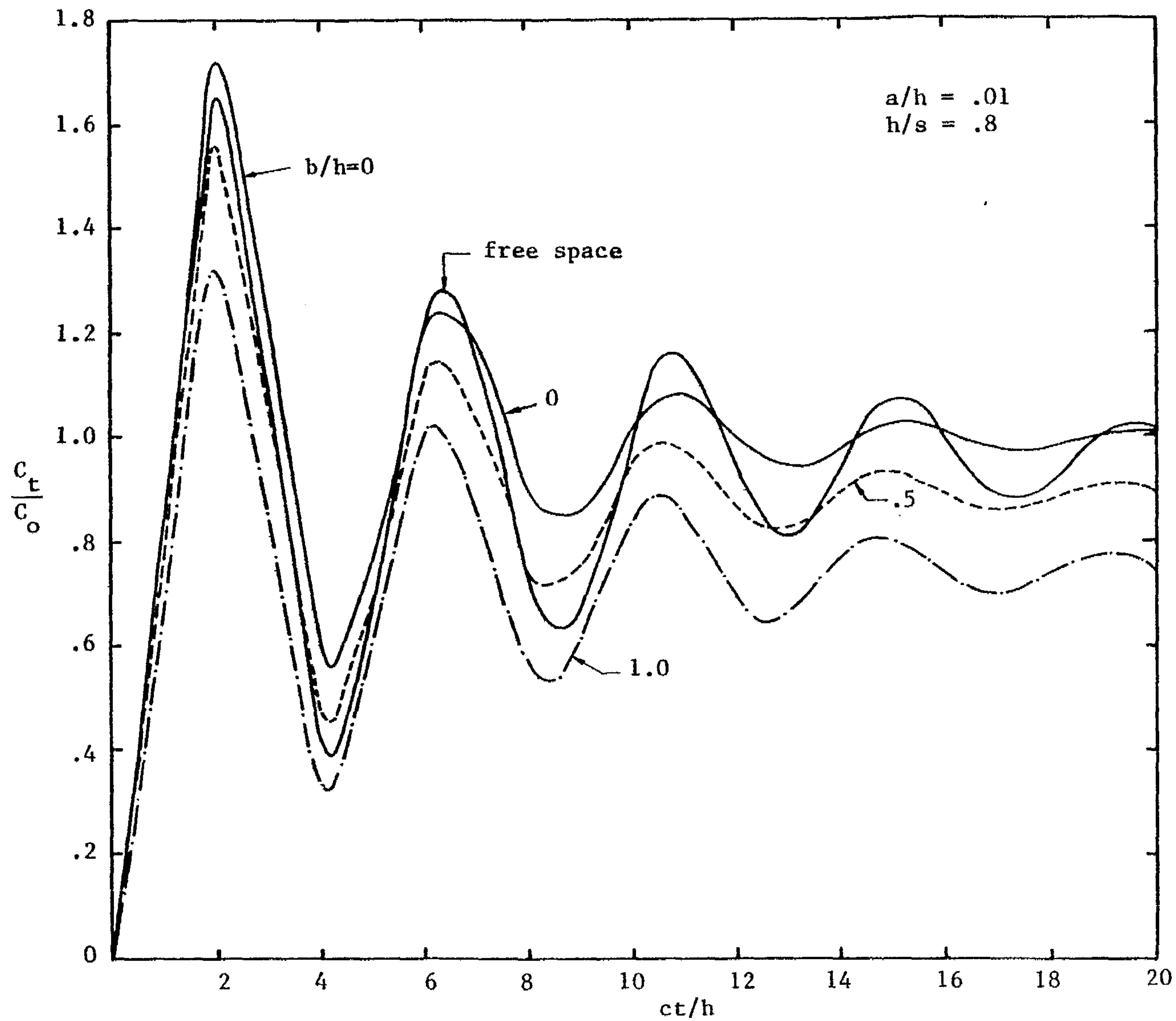

Figure 13. Time history of surface charge density at the post's end with hole radius as parameter.

References

1. R. W. Latham, K. S. H. Lee, and R. W. Sassman, "Minimization of current distortion on a cylindrical post piercing a parallel-plate waveguide," Sensor and Simulation Notes, No. 93, September 1969.
2. R. W. Latham and K. S. H. Lee, "Electromagnetic Interaction Between a Cylindrical Post and a Two-Parallel-Plate Simulator, I," Sensor and Simulation Notes, No. 111, July 1970.

SSN 121

Errata Sheet No. 1

K. S. H. Lee, "Electromagnetic Interaction Between a Cylindrical Post and a Two-Parallel-Plate Simulator, II (a Circular Hole in the Top Plate)" SSN 121, November 1970.

On page 9, the values of C_o should be

$$C_o = \text{value of } C_s \text{ in free space} = \begin{cases} 6.12 \text{ for } a/h = .1 \\ 32.38 \text{ for } a/h = .01 \end{cases}$$

Table III should read as follows:

	a/h = .1		a/h = .01	
b/h	C_s/C_o	C_m/C_o	C_s/C_o	C_m/C_o
0	1.94	2.86	2.21	3.58
.25	1.78	2.56	2.13	3.48
.50	1.54	2.24	1.98	3.25
.75	1.37	2.02	1.81	2.98
1.00	1.24	1.81	1.67	2.75
Free Space	1.00	1.55	1.00	1.70

On pages 25 and 27, the ordinates should read $0.63C_k/C_o$ and $0.63C_t/C_o$, respectively, except for the curves labeled "free-space" whose ordinates are respectively C_k/C_o and C_t/C_o.

On pages 26 and 28, the ordinates should read $0.48C_k/C_o$ and $0.48C_t/C_o$, respectively, except for the curves labeled "free-space" whose ordinates are respectively C_k/C_o and C_t/C_o.